

Stable Radicals from Commonly Used Precursors Trichlorosilane and Diphenylchlorophosphine

Sudipta Roy,[†] A. Claudia Stückl,[†] Serhiy Demeshko,[†] Birger Dittrich,^{*,‡} Jann Meyer,[†] Bholanath Maity,[§] Debasis Koley,^{*,§} Brigitte Schwederski,^{||} Wolfgang Kaim,^{*,||} and Herbert W. Roesky^{*,†}

[†]Institut für Anorganische Chemie, Georg-August-Universität, 37077 Göttingen, Germany

[‡]Institut für Anorganische und Angewandte Chemie, Universität Hamburg, 20146 Hamburg, Germany

[§]Department of Chemical Sciences, Indian Institute of Science Education and Research Kolkata, Mohanpur 741246, West Bengal, India

^{||}Universität Stuttgart, Institut für Anorganische Chemie, 70569 Stuttgart, Germany

S Supporting Information

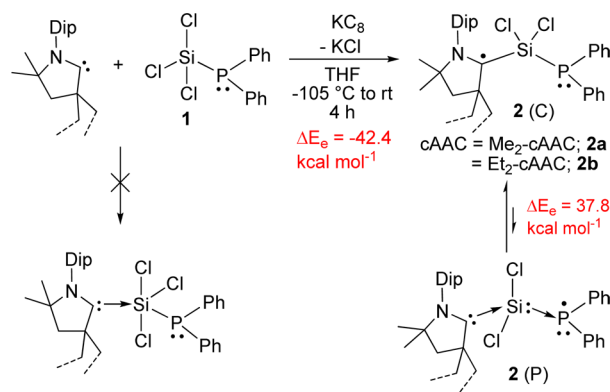
ABSTRACT: Intermediate species dichlorosilylene was generated *in situ* from trichlorosilane and inserted into the P-Cl bond of diphenylchlorophosphine (Ph₂P-Cl) to obtain Ph₂P-SiCl₃ (**1**). Monodechlorination of **1** by cyclic alkyl(amino) carbenes (cAACs)/KC₈ in THF at low temperature led to the formation of stable radicals Ph₂P-Si(cAAC·)Cl₂ (**2a,b**). Compounds **2a,b** were characterized by X-ray single crystal diffraction, mass spectrometry and studied by cyclic voltammetry and theoretical calculations. Radical properties of **2** are confirmed by EPR measurements that suggest the radical electron in **2** couples with ¹⁴N (*I* = 1), ^{35/37}Cl (*I* = 3/2), and ³¹P (*I* = 1/2) nuclei leading to multiple hyperfine lines. Hyperfine coupling parameters computed from DFT calculations are in good agreement with those of experimental values. Electronic distributions obtained from the theoretical calculations suggest that the radical electron mostly resides on the carbene C of **2**.

Radicals and carbenes are very reactive intermediates¹ that play important roles in numerous chemical reactions.² The majority of these two types of intermediate species² are generally produced in low concentrations with a short lifetime. Recently, carbenes were suggested to be suitable ligands toward the stabilization of unstable radical intermediates.³ The halogen derivatives of main group elements are often chosen for the generation of radicals via reductive dehalogenation.⁴ Chlorosilanes are in general important chemical species because of their utilization in industry,^{5a} and they are chemical text book examples as well.^{5b} HSiCl₃ and monoalkyl-substituted chlorosilane (RSiH₂Cl, R = *t*Bu₃Si) react with carbenes (N-heterocyclic carbene, NHC) in a 2:1 molar ratio to produce stable silylene, NHC→SiCl₂, and NHC→SiHR, respectively, under elimination of NHC·HCl.⁶ This synthesis approach facilitates the development of compounds with low-valent Si. The above-mentioned stable silylenes can be used to activate small organic molecules.^{7a} Generally, transition-metal-complexes^{7b} are involved in such reactions. The response of tetrachlorosilane (SiCl₄) toward carbenes is little different. They favor the formation of a stable adduct, NHC→SiCl₄,^{7c} that

was utilized as an elegant precursor for the syntheses of low-coordinate silylenes [(NHC→SiCl)₂ and (NHC→Si)₂].^{7c} Analogously, NHC forms the NHC→PCl₃ adduct with trichlorophosphine (PCl₃). NHC→PCl₃ was completely dehalogenated to obtain the bisphosphinidene, (NHC→P)₂.^{7d} The electronic structures often dramatically change^{7e} in case of the cyclic alkyl(amino) carbene (cAAC) analogues of the above-mentioned compounds. The affinity of carbene towards Si and P centers has only rarely been studied.⁸ Two decades ago, du Mont et al. reported on the first synthesis route of phosphine-substituted chlorosilane.⁹ Afterward, several other research groups¹⁰ developed various synthesis routes for the preparation of phosphasilenes. However, to the best of our knowledge there are not yet any reports on the stable and isolable radicals of phosphino-chlorosilanes.¹¹ Eventually, we realized that the chemistry of carbene/phosphino-chlorosilane is completely different than that of carbene/SiCl₄ and carbene/PCl₃. Herein, we report on the synthesis, characterization, and theoretical calculations of a carbene-stabilized diphenylphosphino-dichlorosilane radical with the general formula Ph₂P-Si(cAAC·)Cl₂ (**2**, Scheme 1; Me₂-cAAC (**2a**) and Et₂-cAAC (**2b**)).

Precursor Ph₂P-SiCl₃ (**1**) has been synthesized via the insertion reaction of SiCl₂ into the P-Cl bond of Ph₂P-Cl.

Scheme 1. Synthesis Route of Ph₂P-Si(cAAC·)Cl₂ (**2a,b**)



Received: March 6, 2015

Published: March 27, 2015

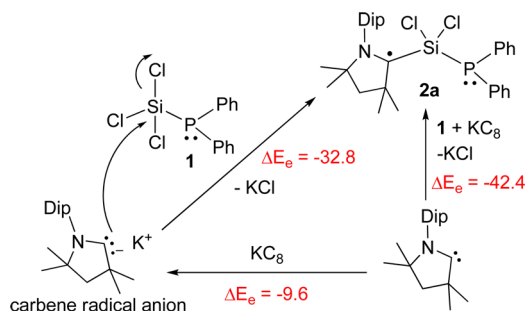


Intermediate species SiCl_2 was generated *in situ*^{12,13} (reacting HSiCl_3 with Et_3N in toluene at a 1:1.1 molar ratio) below -80°C and reacted with Ph_2PCL in 1:1 molar ratio to obtain **1** as a colorless high-boiling liquid in 75% yield. Treatment of **1** with cAAC in the presence of KC_8 in 1:1:1 molar ratio in THF at -105°C to room temperature resulted in the formation of a greenish-red solution. Red blocks/rods of **2** (cAAC = $\text{Me}_2\text{-cAAC}$ (**2a**), $\text{Et}_2\text{-cAAC}$ (**2b**), Scheme 1) were isolated in 22–25% yield.

2a,b were synthesized by controlling the reaction temperature and the molar ratio of the precursor and the reducing agent. A 1:1 molar mixture of cAAC/ KC_8 and one equivalent of **1** were placed separately in two different flasks that were cooled using a liquid nitrogen bath. Precooled THF ($\sim -100^\circ\text{C}$) was added to the flask containing **1** via a canula. The solution of **1** was then passed into the other flask containing cAAC and KC_8 ($\sim -105^\circ\text{C}$). The resultant reaction solution was stirred for 5 min at $\sim -105^\circ\text{C}$ by frequent manual dipping of the flask into liquid nitrogen. At this temperature, no color change was observed. The temperature of the reaction solution was allowed to rise slowly, over 5–10 min; during this time, the color of the slurry changed from colorless to green. This is the crucial part of the synthesis protocol. The green solution was vigorously stirred with occasional manual dipping of the flask into the liquid nitrogen bath (six to eight times over 40–45 min; each dipping for ~ 15 s with manual shaking) to obtain an intensely green solution. The temperature was slowly raised to room temperature (over 30 min), and the resultant solution was stirred (for 3 h at room temperature) to produce a greenish-red solution with deposition of black graphite that was separated by filtration. The filtrate was dried under vacuum and extracted with *n*-hexane. Dark red crystals of **2** are formed in 22–25% yield when the concentrated *n*-hexane solution is stored in a refrigerator (0°C). Crystals of **2** are separated by filtration and washed with a flash of *n*-hexane inside the glovebox and dried under vacuum. **2a,b** are further purified via recrystallization at -32°C from THF or toluene (**2a**) and *n*-hexane (**2b**, at 0°C ; see Supporting Information). For comparison, when a similar reaction was carried out with equivalent amount of NHC instead of cAAC, $\text{NHC} \rightarrow \text{SiCl}_2$ was isolated.^{6a}

$[(\text{Me}_2\text{-cAAC})\text{PPh}_2]^+\text{Cl}^-$ (Supporting Information) was obtained as a major product when **1** was directly reacted with $\text{Me}_2\text{-cAAC}$ in a 1:1 molar ratio, suggesting that $\text{Me}_2\text{-cAAC}$ prefers to bind at the P center with the elimination of SiCl_2 . When **1** was treated with KC_8 in THF at room temperature, unreacted **1** is recovered even after 2 days, indicating that the formation of $\text{Ph}_2\text{P-Si}(\cdot)\text{Cl}_2$ is not facile. On the basis of the experimental evidence, a possible mechanism for the formation of **2a** is proposed in Scheme 2, and the energetics are calculated for **2a**.

Scheme 2. Proposed Mechanism for the Formation of **2a**^a



^a ΔE_e (M06-2X/SVP level) given in kcal mol^{-1} .

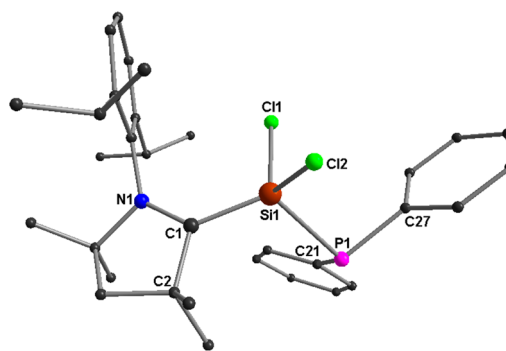


Figure 1. Molecular structure of **2a**. H atoms are omitted for clarity. Selected experimental bond lengths, calculated at the M06-2X/def2-SVP level of theory and given in angstrom, and angles given in degrees: Si1-C1 1.826(3) [1.842], Si1-Cl1 2.0503(12) [2.078], Si1-Cl2 2.0790(11) [2.096], Si1-P1 2.2643(11) [2.285], C1-N1 1.392(4) [1.382], C1-Si1-P1 116.56(10) [119.42], Cl1-Si1-Cl2 105.37(5) [103.94], P1-Si1-Cl1 109.19(5) [112.02], P1-Si1-Cl2 99.97(4) [97.07], C1-Si1-Cl1 111.62(11) [112.05], C1-Si1-Cl2 113.04(10) [110.17], Si1-P1-C21 103.17(10) [105.71], Si1-P1-C27 99.40(10) [98.45], C21-P1-C27 103.09(13) [105.64].

cAACs are well-known for possessing lower-lying LUMO.^{3,8c} *In situ* formation of a carbene radical anion intermediate (cAAC^-) is favorable by $-9.6 \text{ kcal mol}^{-1}$. cAAC^-K^+ reacts with **1** to produce **2** with the formation of KCl . This step of the reaction is favorable by $-32.8 \text{ kcal mol}^{-1}$. Moreover, the formation of the radical at the carbene carbon is advantageous by $-37.8 \text{ kcal mol}^{-1}$ in comparison to that at the phosphorus atom (Scheme 1).

2a,b are soluble in *n*-hexane, THF, and toluene and are stable at 0°C for several months. Crystals of **2a,b** are stable at room temperature for several months in an inert atmosphere, and decompose to $[(\text{cAAC})\text{PPh}_2]^+\text{Cl}^-$ after several days on exposure to air. **2a,b** melt in the range of $157\text{--}158^\circ\text{C}$ (**2a**) and $122\text{--}123^\circ\text{C}$ (**2b**), and have been further characterized by mass spectrometry (Supporting Information). UV-vis spectra of **2a,b** were recorded in THF which show broad absorption bands at 430 and 435 nm, respectively (Supporting Information).

2a,b are characterized by X-ray single crystal diffraction (for **2b**, see Supporting Information). **2a** crystallizes in the monoclinic space group $P2_1/c$. The central Si atom adopts a near-tetrahedral coordination geometry and is bound to one P, one carbene C, and two Cl atoms (Figure 1). The Si-C_{cAAC} bond distance in **2a** is 1.826(3) Å, which is longer (by ~ 0.12 Å) than that of the C_{cAAC} \rightarrow Si coordinate¹³ bond but close to that of the Si-C single bond,^{14g-i} suggesting a covalent σ -sharing bond between Si and carbene C atoms. The C-N bond distance is 1.392(4) Å, which is close to those values found in carbene-centered radicals.¹⁴ N1 is located 0.12 Å above the C1C4C9 plane. The carbene C atom is almost (0.06 Å above) in the C2Si1N1 plane. All these bond parameters suggest that the radical electron resides on the carbene C atom (Schemes 1 and 2). One Cl atom (Cl2) is oriented nearly parallel to the C2C1N1 plane (angle between C2C1N1 and C1Si1Cl2 = 66.85°). The C1Si1P1 and C2C1N1 planes exhibit an angle of 48.55° , whereas Cl1 is almost located in the C2C1N1 plane (7.82°). Selected bond lengths and bond angles are given in the caption of Figure 1.

DFT calculations of **2a,b** were carried out for the doublet states at the UM06-2X/SVP level of theory (for details, see Computational Details in Supporting Information) to illustrate the electronic structures and bonding. The optimized structure

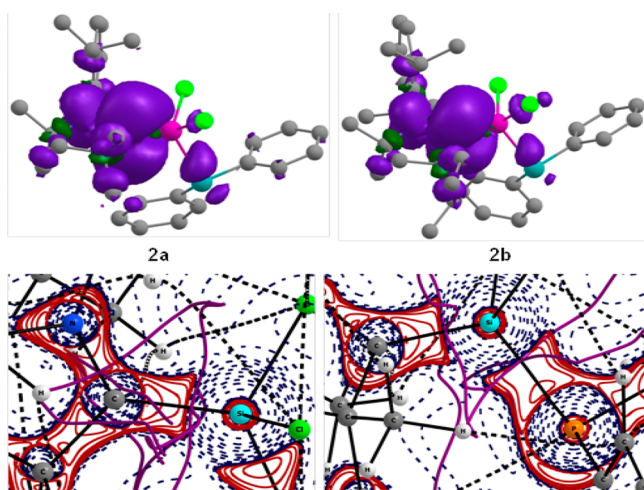


Figure 2. Computed Mulliken spin density (top) of **2a,b** at the UM06-2X/TZVP//UM06-2X/SVP level of theory. Laplacian distribution [$\nabla^2\rho(r)$] in N1-C1-Si1 (bottom left) and C1-Si1-P1 plane (bottom right) of **2a**. Solid lines indicate the areas of charge concentration ($\nabla^2\rho(r) < 0$), whereas dotted lines represent charge depletion ($\nabla^2\rho(r) > 0$). The range of contours of the Laplacian are -8×10^2 to $+8 \times 10^2$. Solid lines connecting atomic nuclei (black) are the bond paths, and those lines separating the atomic basins (purple) indicate the zero-flux surface crossing the molecular plane.

shows strong resemblance to the X-ray crystal structure, as seen from the alignment and superposition of the structure of **2a** (Figure S9). NBO analysis of **2a** entails that the C1 atom is connected with N1, Si1, and C2 via single bonds with occupancies of 1.953, 1.957, and 1.963 e, respectively. The C1 atom contributed $\sim 73\%$ electron density to the C1-Si1 bond, indicating polar character. This result is supported by the properties of the bond critical point (BCP) obtained from AIM (atoms in molecules) calculations. The electron density, $\rho(r)$, at the BCP of C1-N1 (0.294), C1-C2 (0.238), and C1-Si1 (0.119) bonds along with the respective Laplacian ($\nabla^2\rho(r)$; -0.693 , -0.547 , and $+0.316$, respectively) indicates covalent interaction in former two bonds and closed-shell interaction in the last one. However, the calculated ellipticity for C1-Si1 ($\epsilon_{\text{BCP}} = 0.208$) is much lower than that of a C \rightarrow Si donor-acceptor-type bond ($\epsilon_{\text{BCP}} = 0.56$) reported previously,^{14a} indicating its covalent nature. NBO studies also suggest that C1 and P1 atoms contain a LP (lone pair) with an occupancy of 0.866 (single electron, along p_z orbital; considering N1-C1-Si1-C2 lying on xy plane) and 1.882 e, respectively. This is further supported by results obtained from the Laplacian of (3,-3) critical point, called valence-shell charge concentrations (VSCC), shown in Figure 2 (bottom). From the calculated Mulliken spin density plot for **2a,b** shown in Figure 2 (top), it is revealed that the unpaired electron is mostly located on the carbene C (ca. 76% in **2a** and 75% in **2b**, Figure S10), with a comparatively lower contribution from the N1 atom (18% in **2a** and 20% in **2b**) present in the cAAC fragment. Similar results can be perceived by visualizing the SOMO, which is mostly contributed by the C1, Si1, and N1 atoms (Figure S11). It is interesting to note that the unpaired electron exhibits some finite occupancy over Cl2 and P1 centers (Cl2 = $\sim 1\%$ and P1 = $\sim 3\%$ in both **2a,b**). Furthermore, we have calculated the EPR hyperfine coupling constants for **2a,b** at UB3LYP/TZVP level of theory. The calculated hyperfine coupling constant values (A_{iso}) for N1, P1, and Cl2 centers are 4.2, 20.5, and 3.1 G, respectively, of **2a** (for other atoms of **2a**, see Table S6; for **2b**, see Table S7). The

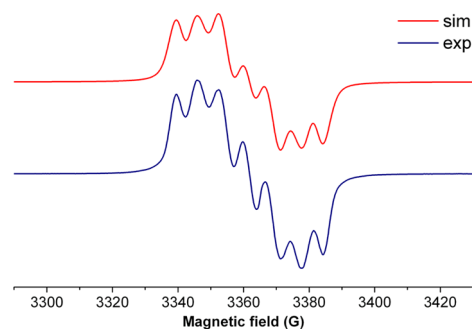


Figure 3. Experimental and simulated EPR spectra of **2a** at 298 K.

calculated values are in good agreement with the simulated/experimental results (vide supra). It is not surprising that the P1 atom shows maximum hyperfine coupling constant (20.54 G in **2a**) because of its parallel alignment with the p_z orbital of the C1 atom. The calculated proton affinities of **2a,b** when one proton binds to the C1 center are 184.1 and 219.2 kcal/mol, respectively.

X-band EPR resonance spectra of **2a,b** were recorded in toluene (Figure 3, for **2b** see Supporting Information). **2a** exhibits a partially resolved EPR spectrum that could be simulated with data according to the DFT-calculated hyperfine coupling: $a(^{31}\text{P})$ 15.6 G (calcd 20.5 G), $a(^{14}\text{N})$ 6.5 G (calcd 4.2 G), $a(^{35}\text{Cl})$ 4.1 G (calcd 3.1 G).

The spin density is mostly concentrated at trivalent C1 (ca. 75%); the adjacent nitrogen center receives about 19% spin density. Accordingly, the g factors for both **2a,b** (2.0027 and 2.0024, respectively) are very close to that of the free electron (2.0023). The heteroatom ^{31}P and one of the Cl atoms in beta position exhibit detectable hyperfine coupling despite rather small spin densities ($< 5\%$). A ^{29}Si satellite coupling (4.7% nat. abundance, $I = 1/2$) could be observed for **2b** at about 10 G (calcd 13.4 G; 3.6% spin density). **2b** contains an apparently mobile ethyl substituent of low symmetry that results in strongly temperature-dependent EPR spectra between 183 and 340 K (Supporting Information) with variable line widths. Although the total spectral width corresponds to that of **2a**, a simulation could thus not be achieved within the accessible temperature range.

Temperature-dependent magnetic susceptibility was measured from 295 to 2 K. The observed $\chi_{\text{M}}T$ product of **2a** at room temperature is $0.32 \text{ cm}^3 \text{ mol}^{-1} \text{ K}$, which is slightly lower than the expected $0.375 \text{ cm}^3 \text{ mol}^{-1} \text{ K}$ for one unpaired electron (with $S = 1/2$), and stays almost constant down to 20 K. Below 20 K, $\chi_{\text{M}}T$ decreases to $0.23 \text{ cm}^3 \text{ mol}^{-1} \text{ K}$, which is likely due to intermolecular antiferromagnetic coupling (Supporting Information).

The redox properties of **2a** were investigated by cyclic voltammetry measurements (Figure 4; for **2b**, see the Supporting Information) that show a one-electron quasi-reversible process at $E_{1/2} = -0.96 \text{ V}$ against $\text{Cp}^*\text{Fe/Cp}^*\text{Fe}^+$, suggesting the formation of anion **2a⁻** (Scheme 3). The calculated one-electron ionization energy and electron affinity of **2a** are 5.3 eV (122.4 kcal/mol; **2a⁺**) and 1.1 eV (26.3 kcal/mol; **2a⁻**), respectively.

In summary, we have developed an elegant synthesis route for the preparation of cyclic alkyl(amino) carbene-stabilized diphenylphosphinodichlorosilane radicals (**2a,b**). These are the first examples of phosphinochlorosilane-containing stable radicals. Crystals of **2a,b** are stable in air for 20 min and for months in an inert atmosphere at room temperature. They are isolated as red blocks (**2a**) or rods (**2b**) and characterized by X-

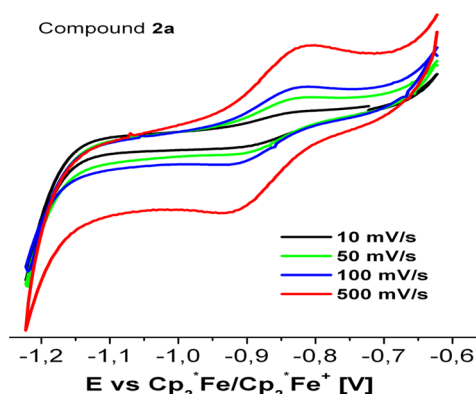
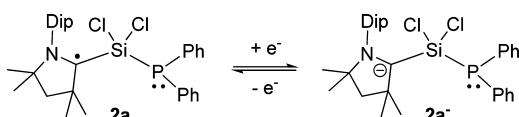


Figure 4. Cyclic voltammogram of a THF solution of **2a** at indicated scan rates, containing 0.1 M $[n\text{-Bu}_4\text{N}]\text{ClO}_4$ as an electrolyte.

Scheme 3. Quasi-Reversible One Electron Reduction of **2a**



ray single crystal diffraction, mass spectrometry, CV, and EPR spectroscopy. Bonding, electronic distributions, and hyperfine electronic interactions of **2a,b** are further studied by theoretical calculations. All the experimental data are in good agreement with the theoretically obtained values.

■ ASSOCIATED CONTENT

Supporting Information

Experimental and theoretical details and characterization data. This material is available free of charge via the Internet at <http://pubs.acs.org>.

■ AUTHOR INFORMATION

Corresponding Authors

*birger.dittrich@chemie.uni-hamburg.de

*koley@iiserkol.ac.in

*kaim@iac.uni-stuttgart.de

*hroesky@gwdg.de

Notes

The authors declare no competing financial interests.

■ ACKNOWLEDGMENTS

H.W.R. thanks the Deutsche Forschungsgemeinschaft (DFG RO 224/60-I) for financial support and Prof. S. Schneider for access to UV-vis measurement. Parts of this research were carried out at the light source Petra III at DESY, a member of the Helmholtz Association (HGF). We would like to thank A. Meents for assistance in using beamline PX11. We thank Wacker Chemie AG for a gift of HSiCl_3 . B.M. thanks CSIR for SRF fellowship, and D.K. thanks IISER-Kolkata for a start-up grant and CSIR for project fund (01(2770)/13/EMR-II). We are thankful to K.C. Mondal for his valuable advices. This paper is dedicated to Manfred Scheer on the occasion of his 60th birthday.

■ REFERENCES

(1) (a) Smith, M. B.; March, J. *Advanced Organic Chemistry*, 5th ed.; Wiley: New York, 2001; Part 1, Chapter 5. (b) Arduengo, A. J., III *Acc. Chem. Res.* **1999**, *32*, 913.

(2) (a) Fuentes, N.; Kong, W.; Fernández-Sánchez, L.; Merino, E.; Nevado, C. *J. Am. Chem. Soc.* **2015**, *137*, 964. (b) Lavallo, V.; Frey, G. D.; Kousar, S.; Donnadiou, B.; Bertrand, G. *Proc. Natl. Acad. Sci. U.S.A.* **2007**, *104*, 13569.

(3) Martin, C. D.; Soleilhavoup, M.; Bertrand, G. *Chem. Sci.* **2013**, *4*, 3020.

(4) (a) Nozawa, T.; Nagata, M.; Ichinohe, M.; Sekiguchi, A. *J. Am. Chem. Soc.* **2011**, *133*, 5773. (b) Nozawa, T.; Ichinohe, M.; Sekiguchi, A. *J. Am. Chem. Soc.* **2012**, *134*, 5540.

(5) (a) Simmler, W. Silicon Compounds, Inorganic. In *Ullmann's Encyclopedia of Industrial Chemistry*; Wiley-VCH: Weinheim, 2000, DOI:10.1002/14356007.a24_001. (b) Holleman, A. F.; Wiberg, E.; Wiberg, N. *Lehrbuch der Anorganischen Chemie*; Walter de Gruyter & Co.: Berlin, 1995.

(6) (a) Ghadwal, R. S.; Roesky, H. W.; Merkel, S.; Henn, J.; Stalke, D. *Angew. Chem., Int. Ed.* **2009**, *48*, 5683; *Angew. Chem.* **2009**, *121*, 5793. (b) Inoue, S.; Eisenhut, C. *J. Am. Chem. Soc.* **2013**, *135*, 18315.

(7) (a) Ghadwal, R. S.; Azhakar, R.; Roesky, H. W. *Acc. Chem. Res.* **2013**, *46*, 444. (b) Díez-González, S.; Marion, N.; Nolan, S. P. *Chem. Rev.* **2009**, *109*, 361. (c) Wang, Y.; Xie, Y.; Wei, P.; King, R. B.; Schaefer, H. F., III; Schleyer, P. v. R.; Robinson, G. H. *Science* **2008**, *321*, 1069. (d) Wang, Y.; Xie, Y.; Wie, P.; King, R. B.; Schaefer, H. F., III; Schleyer, P. v. R.; Robinson, G. H. *J. Am. Chem. Soc.* **2008**, *130*, 14970. (e) Back, O.; Donnadiou, B.; Parameswaran, P.; Frenking, G.; Bertrand, G. *Nat. Chem.* **2010**, *2*, 369.

(8) (a) Hansen, K.; Szilvási, T.; Blom, B.; Inoue, S.; Epping, J.; Dries, M. *J. Am. Chem. Soc.* **2013**, *135*, 11795. (b) Hansen, K.; Szilvási, T.; Blom, B.; Irran, E.; Driess, M. *Chem.—Eur. J.* **2014**, *20*, 1947. (c) Back, O.; Henry-Ellinger, M.; Martin, C. D.; Martin, D.; Bertrand, G. *Angew. Chem., Int. Ed.* **2013**, *52*, 2939; *Angew. Chem.* **2013**, *125*, 3011.

(9) (a) Martens, R.; du Mont, W.-W. *Chem. Ber.* **1992**, *125*, 657. (b) Martens, R.; du Mont, W.-W. *Chem. Ber.* **1993**, *126*, 1115. (c) Zanin, A.; Karnop, M.; Jeske, J.; Jones, P. G.; du Mont, W.-W. *J. Organomet. Chem.* **1994**, *475*, 95. (d) Herzog, U.; Richter, R.; Brendler, E.; Roewer, G. *J. Organomet. Chem.* **1996**, *507*, 221. (e) Müller, L.-P.; du Mont, W.-W.; Jeske, J.; Jones, P. G. *Chem. Ber.* **1995**, *128*, 615. (f) du Mont, W.-W.; Müller, L.; Martens, R.; Papatthomas, P. M.; Smart, B. A.; Robertson, H. E.; Rankin, D. W. H. *Eur. J. Inorg. Chem.* **1999**, 1381. (g) du Mont, W.-W.; Müller, L. P.; Müller, L.; Vollbrecht, S.; Zanin, A. *J. Organomet. Chem.* **1996**, *521*, 417.

(10) See Supporting Information for the contributions from F. Bickelhaupt, E. Niecke, M. Driess, R. Corriu, A. Sekiguchi, A. Baceiredo, C. Cui, D. Scheschkewitz, and S. Inoue.

(11) Pan, X.; Chen, X.; Li, T.; Li, Y.; Wang, X. *J. Am. Chem. Soc.* **2013**, *135*, 3414 and references therein.

(12) Schmeisser, M.; Voss, P. *Z. Anorg. Allg. Chem.* **1964**, *334*, 50.

(13) Roy, S.; Stollberg, P.; Herbst-Irmer, R.; Stalke, D.; Andrada, D. M.; Frenking, G.; Roesky, H. W. *J. Am. Chem. Soc.* **2015**, *137*, 150.

(14) (a) Niepötter, B.; Herbst-Irmer, R.; Kratzert, D.; Samuel, P. P.; Mondal, K. C.; Roesky, H. W.; Jerabek, P.; Frenking, G.; Stalke, D. *Angew. Chem., Int. Ed.* **2014**, *53*, 2766; *Angew. Chem.* **2014**, *126*, 2806.

(b) Kinjo, R.; Donnadiou, B.; Bertrand, G. *Angew. Chem., Int. Ed.* **2010**, *49*, 5930; *Angew. Chem.* **2010**, *122*, 6066. (c) Back, O.; Celik, M. A.; Frenking, G.; Melaimi, M.; Donnadiou, B.; Bertrand, G. *J. Am. Chem. Soc.* **2010**, *132*, 10262. (d) Kinjo, R.; Donnadiou, B.; Celik, M. A.; Frenking, G.; Bertrand, G. *Science* **2011**, *333*, 610. (e) Lavallo, V.; Canac, Y.; Donnadiou, B.; Schoeller, W. W.; Bertrand, G. *Angew. Chem., Int. Ed.* **2006**, *45*, 3488; *Angew. Chem.* **2006**, *118*, 3568. (f) Martin, D.; Moore, C. E.; Rheingold, A. L.; Bertrand, G. *Angew. Chem., Int. Ed.* **2013**, *52*, 7014; *Angew. Chem.* **2013**, *125*, 7152. (g) Mondal, K. C.; Roesky, H. W.; Schwarzer, M. C.; Frenking, G.; Tkach, I.; Wolf, H.; Kratzert, D.; Herbst-Irmer, R.; Niepötter, B.; Stalke, D. *Angew. Chem., Int. Ed.* **2013**, *52*, 1801; *Angew. Chem.* **2013**, *125*, 1845. (h) Mondal, K. C.; Roesky, H. W.; Stückl, A. C.; Ihret, F.; Kaim, W.; Dittrich, B.; Maity, B.; Koley, D. *Angew. Chem., Int. Ed.* **2013**, *52*, 11804; *Angew. Chem.* **2013**, *125*, 12020. (i) Mondal, K. C.; Dittrich, B.; Maity, B.; Koley, D.; Roesky, H. W. *J. Am. Chem. Soc.* **2014**, *136*, 9568.